IEEE Access
Multidisciplinary | Rapid Review | Open Access Journal

Received March 22, 2021, accepted March 29, 2021, date of publication March 31, 2021, date of current version April 9, 2021.

Digital Object Identifier 10.1109/ACCESS.2021.3070155

Optimal Smart Inverter Control for PV and BESS to Improve PV Hosting Capacity of Distribution Networks Using Slime Mould Algorithm

TEKE GUSH, (Graduate Student Member, IEEE), CHUL-HWAN KIM, (Senior Member, IEEE), SAMUEL ADMASIE, (Graduate Student Member, IEEE), JI-SOO KIM, (Graduate Student Member, IEEE), AND JIN-SOL SONG, (Graduate Student Member, IEEE)
Department of Electrical and Computer Engineering, Sungkyunkwan University, Suwon 16419, Republic of Korea

Corresponding author: Chul-Hwan Kim (chkim@skku.edu)

This work was supported by the National Research Foundation of Korea (NRF) grant funded by the Korea government (MSIP) (No. 2018R1A2A1A05078680).

ABSTRACT In this study, an optimal reactive power (Volt/VAr) control of smart inverters for photovoltaic (PV) and battery energy storage systems (BESSs) to improve the PV hosting capacity (PVHC) of distribution networks is proposed. The primary objective of the proposed method is to improve the PVHC of a distribution network by determining the optimal oversize, dispatch, and control setting of the Volt/VAr functions of the smart inverters for both PVs and BESSs. Concurrently, the optimal locations of the PVs and BESSs are determined. The problem is formulated as a multi-objective mixed-integer nonlinear optimization to maximize the PVHC and minimize the voltage deviation simultaneously. A bio-inspired metaheuristic optimization method, i.e., the slime mould algorithm (SMA), is employed to solve the optimization problem. To assess the efficacy of the proposed PVHC improvement method, extensive simulations are conducted on an IEEE 33-node system using MATLAB software. The simulation results verify that the proposed method improves the PVHC of the distribution network compared to different cases and the default Volt/VAr control settings of the smart inverters. Furthermore, the SMA optimization method provides superior performance in finding the optimal PVHC of a distribution network compared to the conventional metaheuristic optimization methods.

INDEX TERMS Distributed energy resources, distribution network, hosting capacity, smart inverter, slime mould algorithm, Volt/VAr control.

NOMENCLATURE

ACRONYMS

BESS	Battery energy storage systems
DER	Distributed energy resource
DNO	Distribution network operator
HC	Hosting capacity
OLTC	On-load tap changers
OS	Over size
PVHC	PV hosting capacity
PV	Photovoltaic
SI	Smart inverter
SMA	Slime mould algorithm
SOC	State of charge
SVC	Static VAr compensator
VD	Voltage deviation
VVCS	Volt/VAr control setting

INDICES

i	Index of system buses $\forall i \in N_b$
j	Index of system buses $\forall j \in N_b$
k	Index of PV system
t	Index of time

PARAMETERS AND VARIABLES

$\delta_{i/j}$	The voltage angles at buses i *or* j
$\eta_{ch/dis}$	Charging/discharging efficiencies of a BESS
ω	The weighted factor
σ	Binary decision variables

The associate editor coordinating the review of this manuscript and approving it for publication was Guijun Li.

θ_{ij}	Impedance angle of the line between bus *i and j*
d	Dead band
E_B	Battery energy
F_1	The objective function of maximization of the total PVHC
F_2	The objective function of minimization of the total VD
I_{MPP}	Current at the maximum power point
I_{SC}	Short-circuit current
K_i	Current temperature coefficient
K_v	Voltage temperature coefficient
m	Slope
N_b	Bus number
N_{PV}	Number of PV systems
N_{total}	Total number of modules
N_T	Total time
$NOCT$	Nominal operating cell temperature
OF	The total multi-objective function
P_{BESS}	The active power for the charging or discharging of a BESS
$P_{ch/dis}$	Charging/discharging power of a BESS
P_D	The active power demand
P_{PV}	Output power of the PV
$P^M_{PV_k}$	The daily maximum active output power of the PVs
Q_D	The reactive power demand
$Q_{PV/BESS}$	The reactive power from the PV/BESS smart inverters
S_{ird}	Solar irradiance
$S_{PV(OS)/BESS(OS)}$	The apparent power of oversized smart inverter for PV/BESS
T_{amb}	Ambient temperature
T_{cell}	Cell temperature
$UB_{ch/dis}$	Maximum active power limit for the charging/discharging
$V^{min/max}$	Minimum/maximum value of voltage
V_{MPP}	Voltage at maximum power point
V_{OC}	Open circuit voltage
$V_r(v_r)$	Reference voltage
W	Weight of slime mould
X	Optimal location of slime mould
Y_{ij}	Element of the Y-bus matrix

I. INTRODUCTION

The penetration of distributed energy resources (DERs), particularly photovoltaic (PV) systems in distribution networks, has been increasing with the growing demand for reliable, sustainable, and clean energy. The efficient penetration of PV systems in a distribution network can provide system stability, power reliability, and quality improvement and can reduce energy losses [1]. Nevertheless, there are technical constraints that arise due to the increasing penetration of PV systems in the distribution network, such as an under/overvoltage, reverse power flow, overloading of feeders and transformers, and protection problems [2]–[4]. These constraints limit the maximum deployment of PVs in the distribution network, which is called the PV hosting capacity (PVHC) of the distribution network. The PVHC is a measure of the maximum amount of PVs that the network can accommodate without negatively impacting on the power quality and reliability of the distribution network [5]. An assessment of the PVHC in the distribution network has significant advantages for distribution network operators, DER owners, and consumers. The PVHC of the distribution network has been enhanced by network augmentation, network reconfiguration, and using different external devices to maintain the technical constraints within the permissible limit. One of the main constraints that limit the PVHC of a distribution network is the increase in voltage due to the high penetration of the PVs. Therefore, optimal voltage regulation can improve the PVHC of the distribution network. Conventionally, the voltage is regulated using on-load tap changers (OLTCs), voltage regulators, and switched capacitors. However, these devices have a limited number of switches and slow response times.

The new IEEE standards (IEEE 1547-2018) suggest that inverter-interfaced DERs can actively participate in grid support functions, such as voltage and frequency regulations [6]. The voltage regulation functionalities of the smart inverters are obtained by operating either active power control or reactive power control function modes [7]. The active power (Volt/Watt) control functions of the smart inverter regulate the local voltage by curtailing the active power. However, this function mode wastes energy and revenue and should be used as infrequently as possible. The reactive power control functions of the smart inverter regulate the local voltage by supplying or absorbing reactive power. It operates in different modes, including constant power factor mode, constant reactive power mode, active power reactive power mode (Watt/VAr), and voltage-reactive power mode (Volt/VAr). In the Volt/VAr reactive power function mode, the smart inverter supplies or absorbs reactive power as a function of the local bus voltage using a predefined Volt/VAr control setting curve. The reactive power outputs and voltage regulation capability of the Volt/VAr mode of the smart inverters depend on the control setting curve. Hence, determining the optimal control of the Volt/VAr setting of the smart inverters can further improve the PVHC of a distribution network.

Battery energy storage systems have been a viable option for voltage regulation, smoothing the intermittent power output of PVs, peak load shaving, and reducing power losses and line loading in distribution networks [8], [9]. However, the BESS has provided these services by only controlling the active power. The BESS provides a further ancillary service by controlling the reactive power of the smart inverter in the BESS and by selecting the optimal BESS size, power dispatch, and locations in the distribution networks [10]. The smart inverter functionality and interoperability of the BESS are tested in [11]. Therefore, a smart inverter for the BESS can provide grid support functionality similar to the smart

inverter for the PVs. In this study, the term "smart inverter for a BESS" is used to refer to the bidirectional converter with additional advanced features.

Numerous methods have been studied in the literature to assess and improve the distribution network hosting capacity (HC) [12]. In [13], a stochastic analysis method was conducted to determine the HC of distribution networks. In this study, an active distribution network management method that includes the reactive power control of smart inverters for a PV system was used to improve the HC of the distribution network. In [14], static and dynamic network reconfigurations were used to improve the HC. In [15], the HC of the distribution network was improved using a robust optimal operation of the OLTC and static VAr compensator (SVC). In [16], reactive power control for central battery storage systems was used to improve the HC of the distribution network. This method reveals the effect of the size of the battery storage and inverter units on the HC of a distribution network. However, the coordination effect of the reactive power control of the PVs and BESSs on the HC of a distribution network was not studied in this method. In [17], a probabilistic method for hosting a high PV penetration in a distribution network using optimal oversized smart inverters with Watt/VAr functions was studied. In [18], smart inverter control strategies and a BESS were used to assess the practical margin PVHC. However, the effect of reactive power control of the smart inverter for a BESS on the PVHC of the distribution network was not considered with this method. Metaheuristic optimization methods have recently been used for assessing the optimal HC, such as the particle swarm optimization (PSO) [19], genetic algorithms (GA) [20], coyote optimization algorithm [21], modified African buffalo optimization [22], Grey wolf optimization [23], etc. Although the aforementioned methods assessed and improved the HC of the distribution networks, there is still room for further improvement by addressing the issues mentioned above.

In this paper, a method for improving the PVHC of a distribution network based on the optimal reactive power control of a smart inverter for PVs and BESSs is presented. An optimization approach is used to determine the optimal oversize, dispatch, and control setting of the Volt/VAr functions of the smart inverters for the PVs and BESSs. In addition, the optimal locations, sizes, and power dispatch for the PVs and BESSs are determined simultaneously. The problem is formulated as a multi-objective optimization method with the objective of maximizing the PVHC and minimizing the voltage deviation (VD) at the same time. A swarm intelligence-based metaheuristic optimization method, i.e., a slime mould algorithm (SMA), is used to solve the optimization problem. Six test cases were simulated on the IEEE 33-node systems using MATLAB software. The simulation results show that the optimized Volt/VAr functions of the smart inverter for the PVs and BESSs have the highest improvement in the total PVHC of the distribution network.

The main contributions of this study are as follows:

1) Smart inverter control: An optimal size, dispatch, and control setting of the Volt/VAr functions of smart inverters for both PVs and BESSs are determined to improve the PVHC.
2) Optimal allocation of PVs and BESSs in the distribution network: The proposed method determines the optimal locations, sizes, and power dispatches of PVs and BESSs in the distribution network.
3) Improving PVHC and minimizing VD of the distribution network: The proposed method improves the PVHC and minimizes the VD of the distribution network at the same time by optimally coordinating PVs and BESSs smart inverter and determining the optimal locations of PVs and BESSs.

Furthermore, comparisons with the default Volt/VAr control settings and conventional metaheuristic optimization methods show that the proposed method has the maximum improvement in the PVHC of the distribution network.

The rest of the paper is structured as follows: Section II describes the modeling of solar irradiance, PV systems, BESS, and smart inverter. The proposed PVHC improvement method is presented in Section III. The problem formulation and the SMA optimization algorithm are also described in Section III. Section IV presents the simulation results. Finally, the paper is concluded in Section V.

II. SYSTEM MODELING

A schematic diagram of the system is presented in Fig. 1. The studied system consists of PV arrays, battery banks, smart inverters for PVs and BESSs, different types of loads, the main grid, and transformers. The active and reactive power flow directions are indicated by the black and red arrows, respectively. The BESS can absorb or supply both active and reactive power, whereas the PV system can supply active power to the system and absorb or supply reactive power. The subsequent subsections thoroughly describe the modeling of solar irradiance, PV systems, BESS, and smart inverters.

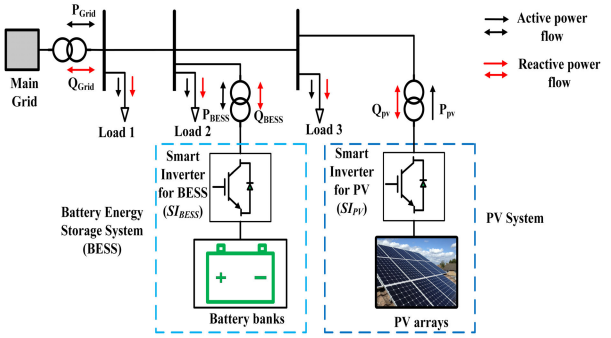

FIGURE 1. Schematic diagram of the studied system.

A. MODELING OF SOLAR IRRADIANCE

The solar irradiance is modeled using a beta distribution to adequately represent variations in solar irradiance [24]. The

probabilistic density function of the beta distribution for $\alpha, \beta \geq 0$, is given as follows:

$$f(S_{ird}|\alpha,\beta) = \begin{cases} \dfrac{\Gamma(\alpha+\beta)}{\Gamma(\alpha)\Gamma(\beta)} \times S_{ird}^{(\alpha-1)} \\ \times (1-S_{ird})^{(\beta-1)}, & for\ 0 \leq S_{ird} \leq 1 \\ 0, & otherwise \end{cases} \tag{1}$$

where Γ is the gamma function and α and β are the shape parameters of the beta distribution. The values of the α and β parameters are estimated using the maximum likelihood estimation from the available data. Subsequently, the Monte Carlo simulation is used to generate samples from the beta distribution.

B. MODELING OF PV SYSTEMS

PV systems consist of PV arrays, which generate power from sunlight, and smart inverters, which convert the DC output power of the PVs into AC power with additional functionalities. The PV output power depends on the solar irradiance and ambient temperature. The calculation for the output power of the PV (P_{pv}) from the solar irradiance and the ambient temperature is described in (2)–(5) [24]:

$$T_{cell} = T_{amb} + \frac{S_{ird}}{0.8} \times (NOCT - 20) \tag{2}$$

$$I_{cell} = S_{ird} \times (I_{sc} + K_i \times (T_{cell} - 25)) \tag{3}$$

$$V_{cell} = V_{oc} - K_v \times T_{cell} \tag{4}$$

$$P_{pv} = N_{total} \times \frac{V_{MPP} \times I_{MPP}}{V_{oc} \times I_{sc}} \times V_{cell} \times I_{cell} \tag{5}$$

C. MODELING OF BESS

The BESSs consist of battery banks, charge controllers, and bidirectional smart inverters. Batteries are the primary component of a BESS, which stores electrical energy in the form of chemical energy. The state of charge (SOC) of the battery, which indicates the available energy in the battery, can be calculated as follows:

$$SOC_i(t) = SOC_i(t-1) + \begin{pmatrix} \dfrac{\sigma_i \eta_{ch_i} P_{ch_i}(t)}{E_{B_i}} \\ -\dfrac{(1-\sigma_i) P_{dis_i}(t)}{\eta_{dis_i} E_{B_i}} \end{pmatrix} \Delta t \tag{6}$$

In this study, we use a BESS model that helps to optimally utilize BESS and accurately determine the reactive output power of a BESS smart inverter. The battery banks are assumed to start charging when the total generated power of the PVs is greater than the total load and discharge when the total generated power of the PVs is less than the total load. This helps to charge the batteries during off-peak hours and discharge during peak hours. The battery banks are not charging above the maximum SOC (SOC^{max}) and discharging below the minimum SOC (SOC^{min}). Furthermore, only one complete charging and discharging cycle is executed daily to increase the life span of the batteries. The maximum active power limit for the charging (UB_{ch_i}), discharging (UB_{dis_i}) of the BESS, and the binary decision variables (σ_i) at a given time t can be expressed as (7)–(9) [10]:

$$UB_{ch_i}(t) = \begin{cases} 0, & \text{if } SOC_i(t) = SOC^{max} \\ -P_{ch_i}^{max}, & \text{if } SOC_i(t) + \dfrac{\eta_{ch_i} P_{ch_i}^{max}}{E_{B_i}} \Delta t \\ & \leq SOC^{max} \quad \forall i, t \\ -E_{B_i} \times (SOC^{max} & \\ -SOC_i(t-1))\Delta t, & \text{if } SOC_i(t) + \dfrac{\eta_{ch_i} P_{ch_i}^{max}}{E_{B_i}} \Delta t \\ & > SOC^{max} \end{cases} \tag{7}$$

$$UB_{dis_i}(t) = \begin{cases} 0, & \text{if } SOC_i(t) \leq SOC^{\min} \\ P_{dis_i}^{max}, & \text{if } SOC_i(t) - \dfrac{P_{dis_i}^{max}}{\eta_{dis_i} E_{B_i}} \Delta t \\ & \geq SOC^{\min} \quad \forall i, t \\ E_{B_i} \times (SOC_i(t) & \\ -SOC^{\min})\Delta t, & \text{if } SOC_i(t) - \dfrac{P_{dis_i}^{max}}{\eta_{dis_i} E_{B_i}} \Delta t \\ & < SOC^{\min} \end{cases} \tag{8}$$

$$\sigma = \begin{cases} 1, & \text{if } \sum_{k=1}^{N_{pv}} P_{PV_k}(t) \geq P_{D_T}(t) \\ 0, & \text{if } \sum_{k=1}^{N_{pv}} P_{PV_k}(t) < P_{D_T}(t) \end{cases} \tag{9}$$

D. SMART INVERTER MODELING FOR PV AND BESS

A smart inverter is used to interface the DC output of the DERs, such as the PVs and BESSs, into the AC grid with additional grid supportive functionality. This functionality includes the adoption of reactive power functions to provide adequate local voltage regulation for a voltage variation caused by the intermittent nature of the DERs. In this study, the Volt/VAr function of a smart inverter for both PVs and BESSs is considered to improve the PVHC of the distribution network.

The Volt/VAr function mode of the smart inverter can provide a certain amount of reactive power as a function of the local voltage according to the control setting curve, as shown in Fig. 2. From this control setting curve, the smart inverter does not supply any reactive power during the dead band (d) range. If the voltage is below v_2, the smart inverter operates in a capacitive mode, thereby supplying reactive power. In addition, if the voltage is above v_3, the smart inverter operates in an inductive mode, thereby absorbing the reactive power. Moreover, when the voltage is between v_1 and v_2 as well as v_3 and v_4, the smart inverter supplies and absorbs reactive power as a function of the slope (m), respectively. Conventionally, the control setting curve points of the smart inverter are set to the default values [25]. In this study, the optimal control setting curve points (v_1, v_2, v_3, and v_4) for both PV and BESS smart inverters are determined based on the dead band

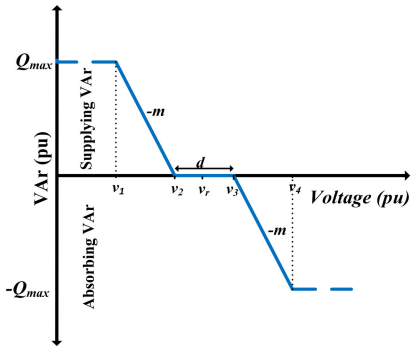

FIGURE 2. Volt/VAr control setting curve.

(d), slope (m), and the reference voltage (v_r), expressed as follows:

$$\begin{aligned} v_1 &= \frac{2 \times m \times v_r - d \times m - 2 \times Q_{\max}}{2 \times m} \\ v_2 &= \frac{2 \times v_r - d}{2} \\ v_3 &= \frac{2 \times v_r + d}{2} \\ v_4 &= \frac{2 \times m \times v_r + d \times m + 2 \times Q_{\max}}{2 \times m} \end{aligned} \tag{10}$$

The Volt/VAr function mode of the smart inverter can generate reactive power using either watt priority or VAr priority modes. During the watt priority mode, the active power is prioritized over reactive power generation. Therefore, the smart inverter does not generate reactive power when the smart inverter absorbs or supplies active power at its full capacity. In the VAr priority mode, the reactive power is prioritized over the active power generation. This is implemented by curtailing the active power when there is insufficient headroom for the reactive power in the smart inverter. However, this mode wastes the generated active power. The reactive power output of the smart inverter depends on the active power output and inverter size. Hence, oversizing the inverter can increase the headroom for the reactive power of the smart inverter. The maximum available reactive power from the oversized smart inverter for a PV and a BESS can be expressed as follows:

$$Q_{PV}^{\max} = \sqrt{S_{PV(OS)}^2 - P_{PV}^2} \tag{11}$$

$$Q_{BESS}^{\max} = \sqrt{S_{BESS(OS)}^2 - P_{BESS}^2} \tag{12}$$

where $S_{PV(OS)}$ and $S_{BESS(OS)}$ are the apparent power of the oversized smart inverter for a PV and a BESS, respectively; P_{BESS} is the active power for the charging or discharging of a BESS; and $Q_{PV}^{\max}$ and $Q_{BESS}^{\max}$ are the maximum reactive power of a PV and BESS, respectively. In this study, the watt-priority Volt/VAr function mode of the smart inverter is considered, and the reactive power is generated or absorbed during the day and night for both the PV and BESS smart inverters.

III. PROPOSED PVHC IMPROVEMENT METHOD

This section presents an optimization approach for determining the proposed PVHC improvement method. The PVHC improvement is assessed by acquiring the optimal Volt/VAr function mode of the smart inverter for both PV and BESS. A multi-objective optimization method is utilized to simultaneously establish the maximum PVHC and minimum VD by determining the optimal oversize, dispatch, and control setting of the Volt/VAr functions of the smart inverters for PVs and BESSs. Concurrently, the optimal locations of the PVs and BESSs are also determined. SMA is used to obtain the optimal values of the decision variables for improving the PVHC. The formulation of the problem and the SMA optimization method are described in the subsequent subsections.

A. PROBLEM FORMULATION

The problem of the proposed PVHC improvement method is formulated as a multi-objective mixed-integer nonlinear optimization problem. The considered multi-objective functions and the operational constraints are described as follows:

1) OBJECTIVE FUNCTIONS

Two objective functions were considered in this study. The first objective function (F_1) is the maximization of the total PVHC of the distribution networks, as presented by (13), and the second objective function (F_2) is the minimization of the total VD in the distribution networks, as presented by (14).

$$F_1 = \max\ PVHC = \sum_{k=1}^{N_{PV}} P_{PV_k}^M \tag{13}$$

$$F_2 = \min\ VD = \sum_{t=1}^{N_T} \sum_{i=1}^{N_b} \left(\frac{V_i(t) - V_r}{V_r} \right)^2 \tag{14}$$

where $P_{PV_k}^M$ is the daily maximum active output power of the PVs, N_{PV} is the number of PV systems, k is the PV system index, N_b is the bus number, N_T is the total amount of time, $V_i(t)$ is the magnitude of the voltage at bus i and time segment t, and V_r is the reference voltage for all buses. To solve these two objective functions simultaneously, a weighted sum-based multi-objective optimization method is used as shown in (15).

$$\max OF = \omega_1 F_1 - \omega_2 F_2 \tag{15}$$

where ω_1 and ω_2 are the weighted factors for each objective function and the sum of their values should be 1. Selecting different combination values for the weighted factors provides different optimization results. In this study, the weighted factors were selected by trial and error.

2) CONSTRAINTS

The optimization problem is subjected to the following equality and inequality constraints.

$$P_{Grid}(t) + P_{PV_i}(t) \pm P_{BESS_i}(t) - P_{D_i}(t)$$

$$= V_i(t)\sum_{j=1}^{N_b} V_j(t)Y_{ij}\cos(\theta_{ij} + \delta_j(t) - \delta_i(t)) \quad (16)$$

$$Q_{Grid}(t) + Q_{PV_i}(t) \pm Q_{BESS_i}(t) - Q_{D_i}(t) = -V_i(t)\sum_{j=1}^{N_b} V_j(t)Y_{ij}\sin(\theta_{ij} + \delta_j(t) - \delta_i(t)) \quad (17)$$

$$V^{\min} \le V_i(t) \le V^{\max} \quad (18)$$

$$I_{i,j}(t) \le I_{i,j}^{\max} \quad (19)$$

$$P_{PV}^{\min} \le P_{PV_i} \le P_{PV}^{\max} \quad (20)$$

$$E_B^{\min} \le E_{B_i} \le E_B^{\max} \quad (21)$$

$$SOC^{\min} \le SOC_i(t) \le SOC^{max} \quad (22)$$

$$UB_{ch_i}(t) \le P_{BESS_i}(t) \le UB_{dis_i}(t) \quad (23)$$

$$SOC(N_T) - SOC(0) \le \varepsilon \quad (24)$$

$$S_{PV(os)}^{\min} \le S_{PV(os)} \le S_{PV(os)}^{\max} \quad (25)$$

$$S_{BESS(os)}^{\min} \le S_{BESS(os)} \le S_{BESS(os)}^{\max} \quad (26)$$

$$m^{\min} \le m \le m^{\max} \quad (27)$$

$$d^{\min} \le d \le d^{\max} \quad (28)$$

where (16) and (17) represent the power balance constraint at each node. In addition, P_{Grid} and Q_{Grid} are the active and reactive power of the grid at the slack bus, respectively; Q_{PV_i} and Q_{BESS_i} are the reactive power from the PV and BESS smart inverters at bus i and time t, respectively; P_{D_i} and Q_{D_i} are the active and reactive power of demand at bus i and time t, respectively; Y_{ij} is the element of the Y-bus matrix; θ_{ij} is the impedance angle of the line between bus i and j; and δ_j and δ_i are the voltage angles at buses j and i, respectively. Equation (18) indicates that the voltage at each node must be within the minimum voltage (V^{min}) and maximum voltage (V^{max}) limit. The limit of the current carrying capacity (ampacity) of the line between buses i and j is given in (19). Equations (20) and (21) represent the integration limit of PVs power and BESS energy at bus i, respectively. Equations (21)–(24) describe the BESS constraints. The difference between the SOC at an N_T time interval and the initial SOC should be minimized to fully utilize one complete charging and discharging cycles daily. Equations (25)–(28) express the constraints of the smart inverter for both PVs and BESSs. The oversized smart inverters for PV and BESS ($S_{PV(OS)}$ and $S_{BESS(OS)}$) are limited between the minimum ($S_{PV(os)}^{\min}$ and $S_{BESS(os)}^{\min}$) and maximum ($S_{PV(os)}^{\max}$and $S_{BESS(os)}^{\max}$) values as shown in (25) and (26), respectively. The slope (m) and dead band (d) of the Volt/VAr control setting of the smart inverter for both PV and BESS are limited to the minimum (m^{min} and d^{min}) and maximum (m^{max} and d^{max}) values as shown in (27) and (28), respectively.

B. SLIME MOULD ALGORITHM

The SMA is a new biologically inspired metaheuristic optimization method proposed in [26]. The SMA mimics the foraging of slime mould to find the optima of the problem. The slime mould searches for food by producing a propagation wave based on bio-oscillations, creating the optimal route for connecting food. The SMA mathematically expresses the slime mould food searching ability using adaptive weights that simulate the slime mould bio-oscillator. The food approach behavior of a slime mould can be imitated through the following mathematical expression:

$$X(l+1) = \begin{cases} rand \cdot (UB - LB) + LB, & rand < y \\ X_b(l) + u_b \cdot (W \cdot X_A(l) - X_B(l)), & r < p \\ u_c \cdot X(l), & r \ge p \end{cases} \quad (29)$$

Here, LB and UB are the lower and upper bound, respectively, r and $rand$ are the random numbers between [0, 1], and y is the constant parameter. The parameter u_b is within a limit of [-a, a], u_c decreases linearly from 1 to 0, in which l denotes the current iteration, and X and X_b are the location of the slime mould and the location of the individual slime mould with the highest odor concentration, respectively. In addition, X_A and X_B denote randomly selected individuals from the swarm and W is the weight of slime mould. The value of p is given by (30).

$$p = \tanh|S(z) - D_F| \quad (30)$$

where z ∈ 1,2,…,n, $S(z)$ and D_F are the fitness of X, and the best fitness obtained in all iteration, respectively. the value of u_b obtained as follows:

$$u_b = [-a,\ a] \quad (31)$$

$$a = \operatorname{arctanh}\left(-\left(\frac{l}{\max_l}\right) + 1\right) \quad (32)$$

The positive and negative feedback between the slime mould vein width and food concentration is simulated mathematically as follow:

$$W(SmellIndex(l)) = \begin{cases} 1 + r\log\left(\frac{b_F - S(z)}{b_F - w_F} + 1\right), & condition \\ 1 - r\log\left(\frac{b_F - S(z)}{b_F - w_F} + 1\right), & others \end{cases} \quad (33)$$

$$SmellIndex = sort(S) \quad (34)$$

Here, b_F and w_F are the best and worst fitness values during the current iterative process, respectively, r is a random number between [0, 1], *condition* indicates that $S(z)$ ranks the first half of the population, *SmellIndex* denotes the sorted fitness values. The SMA pseudo-code is presented in Algorithm 1.

The SMA is selected to solve the proposed optimization problem because it is simple, requires few parameters, has an excellent searching ability and exploitation propensity, and is applicable for a large number of decision variables and multiple objective functions. Moreover, it achieves high performance and robustness in determining globally optimal values compared with the existing metaheuristic algorithms [27].

Algorithm 1 Pseudo-Code of SMA [26]

Initialize the population size and max iteration (max_l);
Initialize the position of slime mould X_z(z=1,2,...,n);
While ($l \leq max_l$)
  Calculate the fitness of all slime mould;
  Update bestFitness, X_b;
  Calculate the W by **Eq.**(33);
  For each search portion
  Update p, u_b, u_c;
  Update position by **Eq.**(29);
  End For
  l=l+1;
End While
Return bestFitness, X_b;

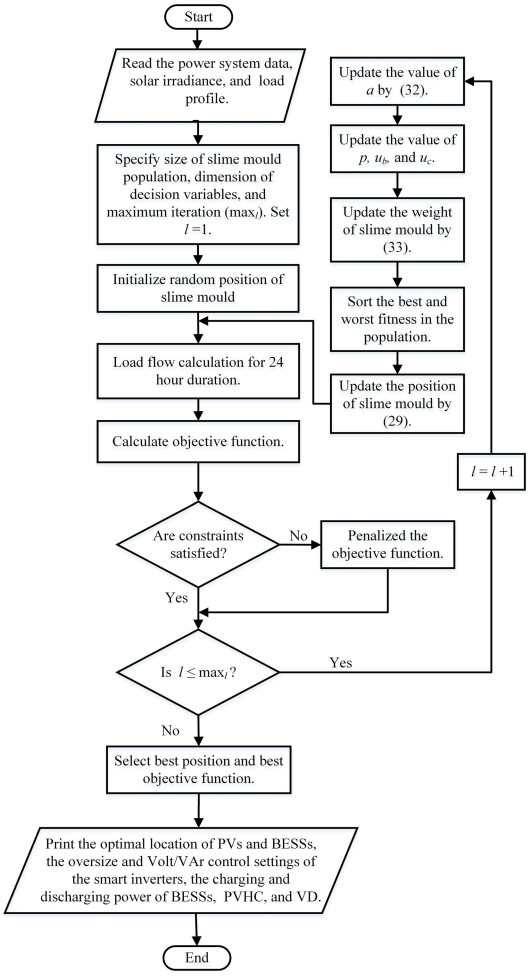

FIGURE 3. Flowchart of the proposed method.

A flowchart representation of the proposed method is shown in Fig. 3. The flowchart of the proposed method can be explained as follows. First, the data, such as the power system data, the solar irradiance, and load data are collected. Then, the SMA maximum population, decision variables, and maximum iterations (max_l) are specified for the optimization process and initialize the random positions of the slime mould. The SMA search agent can be represented as vector X_z whose elements are the values of the decision variable i.e., location of PVs and BESSs, the oversize and Volt/VAr control settings of the smart inverters, and the charging and discharging power of BESSs. This search agent represents the position of the slime mould. Then, apply the load flow calculation for the 24-h duration and check the constraints are within the limit in each time interval. If the constraints are not met, the objective function will be penalized. Subsequently, the value a, p, u_b, u_c, and W of SMA are updated as given in (30–33) until the maximum iteration is reached. In each iteration, the objective function is estimated for each of the slime mould and the best position is updated as given in (29). Finally, select the best position of slime mould, i.e., location of PVs and BESSs, the oversize and Volt/VAr control settings of the smart inverters, and the charging and discharging power of BESSs, which give the best objective function i.e., maximum PVHC and minimum VD.

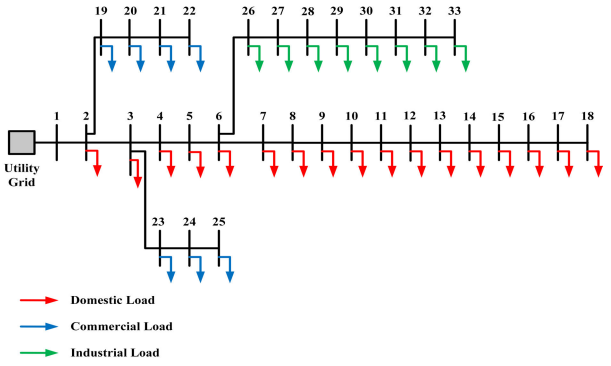

FIGURE 4. IEEE 33-node distribution test system.

TABLE 1. The values of parameters used in the optimization algorithm.

Parameters	Values
Population size	100
Maximum iteration	100
N_T	24 hours
Weighted factors (ω_1 and ω_2)	0.5
V^{min} and V^{max}	0.95 and 1.05 pu
η_{ch_i} and η_{dis_i}	0.9
SOC^{min} and SOC^{max}	0.1 and 1
$P^{max}_{ch_i}$ and $P^{max}_{dis_i}$	1 MW
E^{max}_B and P^{max}_{PV}	6.5 MWh and 10 MW
$S^{min}_{PV(OS)}$ and $S^{min}_{BESS(OS)}$	10%
$S^{max}_{PV(OS)}$ and $S^{max}_{BESS(OS)}$	100%
m^{min} and m^{max}	0.2 and 1
d^{min} and d^{max}	0 and 0.1

IV. SIMULATION RESULTS

Extensive simulations were conducted using MATLAB software to demonstrate the effectiveness of the proposed PVHC improvement method. The details of the test system, case studies, comparison with the default Volt/VAr control settings

TABLE 2. Simulation results of the optimal size and location of PVs and BESSs, total PVHC, VD, and smart inverter oversize (OS) for PVs and BESSs.

Cases	PV No.	Optimal location of PVs	$P^{M}_{PV_k}$ (MW)	BESS No.	Optimal location of BESS	Energy of BESS (MWh)	Total PVHC (MW)	VD (pu)	$S_{PV(OS)}$ (%)	$S_{BESS(OS)}$ (%)
1	—	—	—	—	—	—	—	1.1783	—	—
	PV_1	28	0.8379	—	—	—			92.89	—
2	PV_2	2	6.6482	—	—	—	7.9150	0.0637	20.15	—
	PV_3	14	0.4288	—	—	—			85.39	—
	PV_1	3	5.4919	$BESS_1$	12	4.5339			—	—
3	PV_2	16	1.0760	$BESS_2$	9	4.1266	8.3459	0.2504	—	—
	PV_3	31	1.7780	—	—	—			—	—
	PV_1	13	0.4112	$BESS_1$	4	5.2626			98.05	—
4	PV_2	2	7.4155	$BESS_2$	23	4.6848	8.5991	0.0602	20.63	—
	PV_3	30	0.7724	—	—	—			95.00	—
	PV_1	3	4.6058	$BESS_1$	5	5.0769			—	66.45
5	PV_2	30	1.8489	$BESS_2$	8	5.3903	8.6838	0.0526	—	92.81
	PV_3	19	2.2291	—	—	—			—	—
	PV_1	3	8.4063	$BESS_1$	24	4.7152			23.36	22.93
6	PV_2	31	0.4616	$BESS_2$	11	5.3548	**9.2833**	**0.0139**	95.89	54.01
	PV_3	12	0.4153	—	—	—			74.30	—

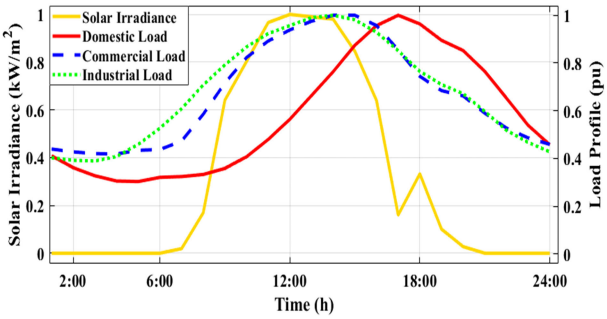

FIGURE 5. Hourly sampled solar irradiance and load profile data.

and with conventional metaheuristic optimization methods are described in the subsequent sections.

A. TEST SYSTEMS

The IEEE 33-node test system was used to assess the efficacy of the proposed PVHC improvement method. This test system operates at a base voltage of 12.66 kV and a base apparent power of 10 MVA. This test system has 33-buses, 3 laterals, and 32 branches. Detailed specifications of the line and bus data of the IEEE 33-node system were obtained from [28]. The single-line diagrams of the IEEE 33-node systems along with the assigned load types are demonstrated in Fig. 4. Loads of the IEEE 33-node test systems are assigned based on the daily residential, commercial, and industrial load profiles during summer with a 1-h interval obtained from [29]. To determine the uncertain solar irradiance samples, hourly summer solar irradiance data of 5 years (2015–2019) obtained from the National Renewable Energy Laboratory (NREL), National Solar Radiation Database (NSRDB) [30] were used in this study. Fig. 5 illustrates the hourly sampled solar irradiance and load profile data.

As suggested in [31], three distributed PVs are selected as the optimal number of PVs for the IEEE 33-node test system. The parameters of the PV module are obtained from [9]. The total number of modules is determined optimally for each PV to determine the optimal size of the PVs integrated into the test system. Two distributed BESSs are selected as the economical and optimal number of BESSs for the IEEE 33-node test system. The PVs and BESSs are integrated as a negative load and can connect to all buses except bus 1 (slack bus). The backward/forward sweep load flow method was used to solve the load flow equation. The minimum and maximum voltage magnitudes across all buses are considered within the ANSI standard limit (0.95 pu $\leq V \leq$ 1.05 pu). The maximum current carrying capacity limit of each branch of the IEEE 33-node test system is obtained from [32]. The maximum active and reactive power exchange with the upstream utility grid is 6 MW and 3 MVAr, respectively. Table 1 summarizes the values of the parameters used in the optimization algorithm.

B. CASE STUDIES

Six cases were executed in the IEEE 33-node test system to verify the effectiveness of the proposed method. The first case (case 1) represents the base case where PV and BESS are not integrated into the test system. Cases 2 and 3 examine the PVHC of the test system by optimally controlling the smart inverter for the PVs and by optimally integrating the BESSs, respectively. In case 3, the reactive power function of the smart inverter is not considered for both the PVs and the BESSs. In case 4, the PVHC of the test system is examined using BESSs and optimal smart inverter control for only the PVs. In case 5, the PVHC of the test system is investigated using BESSs and optimal smart inverter control for only the BESSs. In case 6, the optimal smart inverter control for both PVs and BESSs is used to improve the PVHC of the test system.

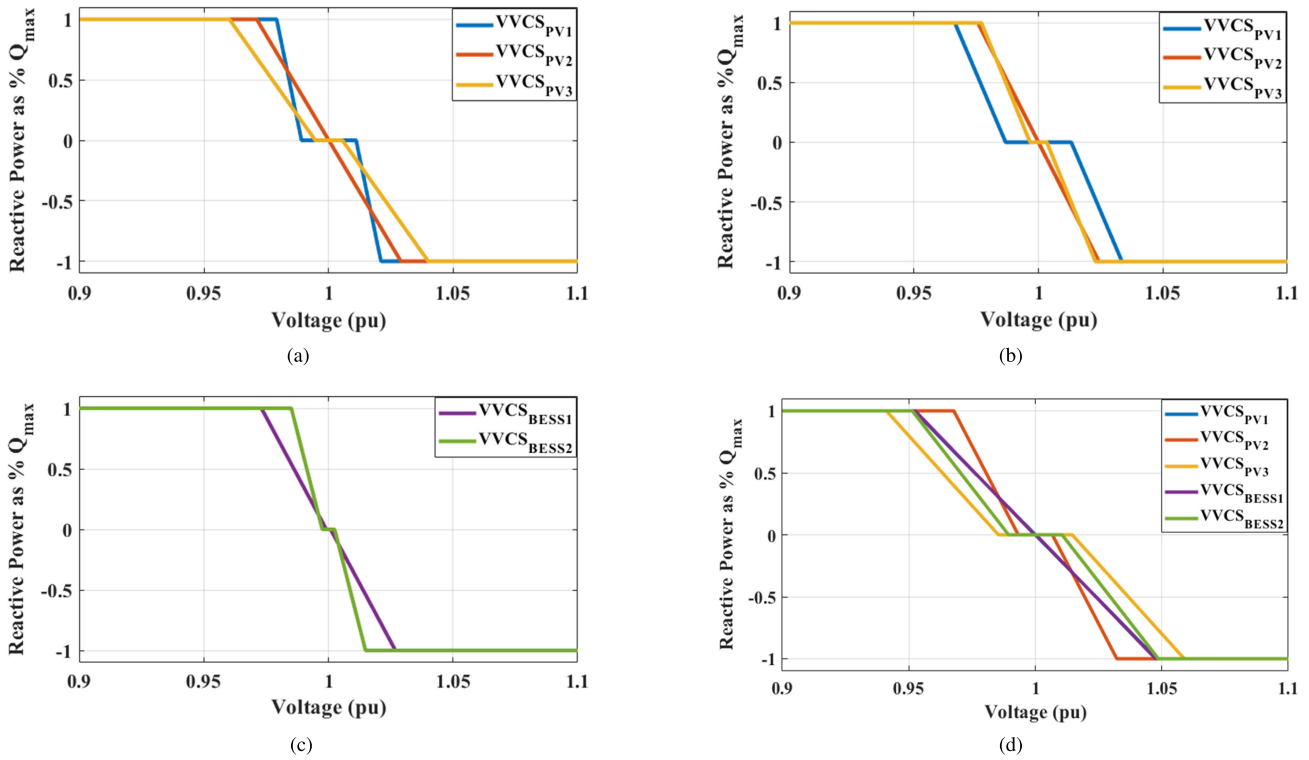

FIGURE 6. Optimal Volt/VAr control setting (VVCS) of smart inverters for (a) case 2, (b) case 4, (c) case 5, and (d) case 6.

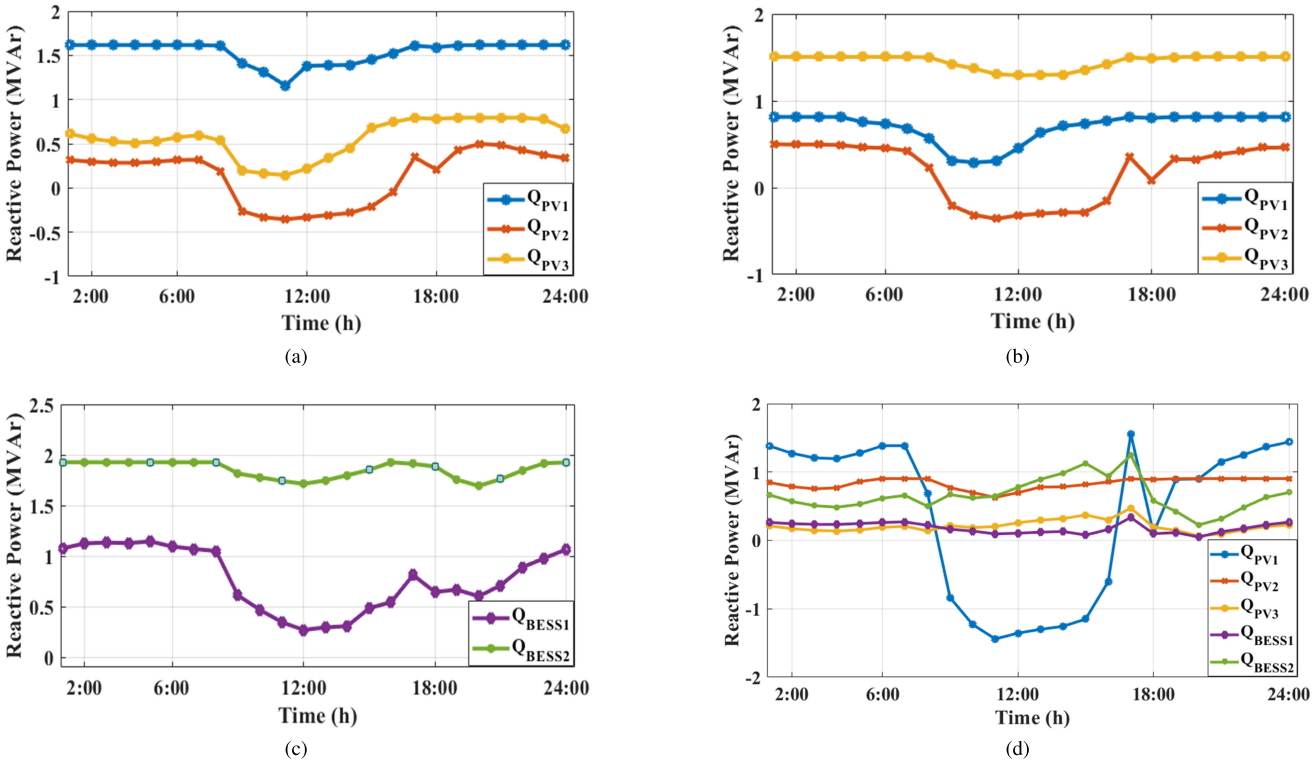

FIGURE 7. Reactive power (Q) output of smart inverters at the optimal location for (a) case 2, (b) case 4, (c) case 5, and (d) case 6.

Table 2 presents the simulation results obtained for each case. Case 1 shows the VD of the IEEE 33-node test system without integrating the PVs and BESSs. It can be observed that the optimal integration of PVs with optimal smart inverter control in case 2 reduced the VD in comparison with that in case 1. The results of case 3 show that the PVHC is

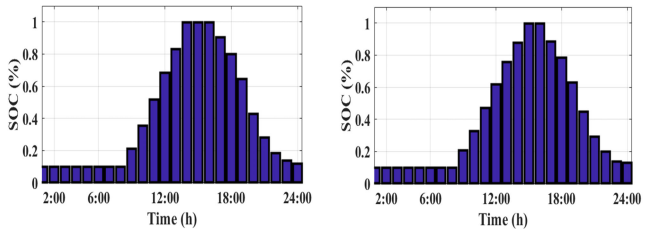

FIGURE 8. Hourly state of charge (%) for (a) $BESS_1$ and (b) $BESS_2$ at optimal location of the test system for case 6.

improved, whereas the VD is increased compared with that of case 2. The optimal integration of the BESSs and optimal smart inverter control for the PVs in case 4 further improved the PVHC and minimized the VD compared to those in cases 2 and 3. The results of case 5 show that using the BESSs with optimal smart inverter control improves the PVHC and minimizes the VD compared with cases 2–4. The case proposed in this study is case 6, which determined the PVHC and VD by finding the optimal location, Volt/VAr control setting, and by oversizing the smart inverter for both PVs and BESSs. The results show that case 6 exhibited the highest improvements in the PVHC and minimum VD in comparison with the other cases.

Fig. 6 shows the optimal Volt/VAr control setting for each smart inverter of the PVs and BESSs for cases 2, 4, 5, and 6, respectively. It can be seen that the control setting for each smart inverter is autonomously determined based on the local voltage. Fig. 7 shows the reactive power output of the smart inverter for the PVs and BESSs at the optimal location on the test system for cases 2, 4, 5, and 6, respectively. It was observed that the smart inverters for the PVs and BESSs also provides reactive power during night time and when there is no charge or discharge of the BESSs. This shows that the smart inverter for the PVs and BESSs can operate as a STATCOM at night and during the ideal time period.

Fig. 8 shows the status of the hourly SOC for the two distributed BESSs at the optimal location of the test system in case 6. The figure shows that both distributed BESSs are charged during a high generation of PVs and discharged during on-peak load hours, providing peak shaving. Fig. 9 shows the bus voltage for all buses at each time interval for all cases.

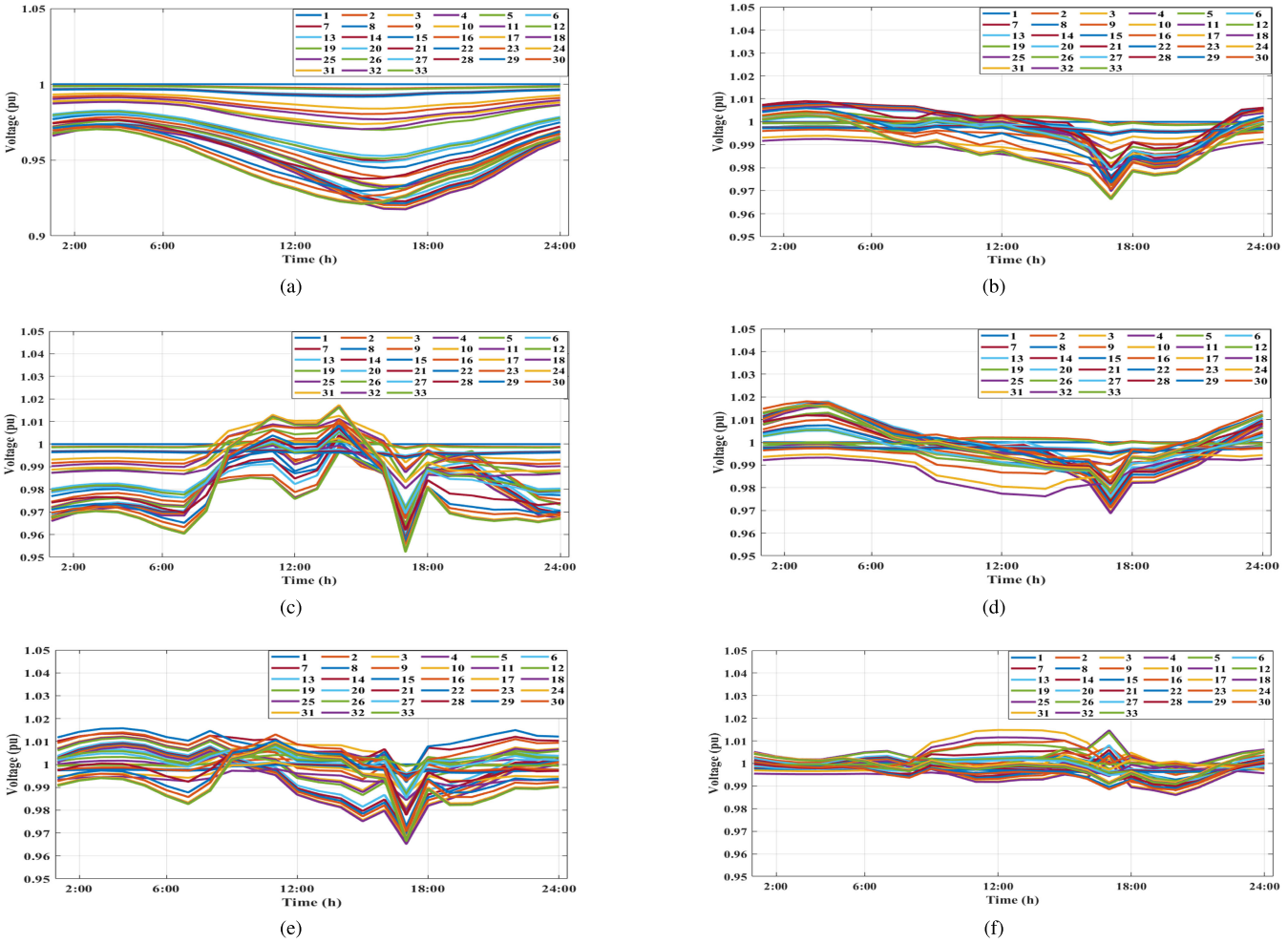

FIGURE 9. The bus voltage for all buses at each time interval for (a) case 1, (b) case 2, (c) case 3, (d) case 4, (e) case 5, and (f) case 6.

TABLE 3. Comparison of optimal Volt/VAr control setting with default Volt/VAr control setting.

Cases	Default Volt/VAr control setting				Optimal Volt/VAr control setting			
	Optimal location of PVs	Optimal location of BESS	Total PVHC (MW)	VD (pu)	Optimal location of PVs	Optimal location of BESS	Total PVHC (MW)	VD (pu)
2	33, 18, and 2	—	7.5752	0.1228	28, 2, and 14	—	7.9150	0.0637
4	32, 3, and 16	9 and 8	8.3993	0.1200	13, 2, and 30	4 and 23	8.5991	0.0602
5	16, 2, and 28	18 and 33	8.5997	0.1328	3, 30, and 19	5 and 8	8.6838	0.0526
6	31, 2, and 15	16 and 33	8.9621	0.0501	3, 31, and 12	24 and 11	9.2833	0.0139

TABLE 4. Comparison with conventional metaheuristic optimization methods.

Cases	Optimal location of PVs			Optimal location of BESSs			Total PVHC (MW)			VD (pu)		
	GA	PSO	SMA	GA	PSO	SMA	GA	PSO	SMA	GA	PSO	SMA
2	10, 30, and 2	33, 9, and 2	28, 2, and 14	—	—	—	7.7991	7.8999	7.9150	0.0839	0.0891	0.0637
3	21, 6, and 27	6, 19, and 2	3, 16, and 31	10 and 28	9 and 13	12 and 9	8.2811	8.2994	8.3459	0.2805	0.2802	0.2504
4	12, 29, and 2	3, 15, and 33	13, 2, and 30	13 and 26	4 and 8	4 and 23	8.4409	8.4782	8.5991	0.0629	0.0610	0.0602
5	19, 4, and 30	5, 16, and 2	3, 30, and 19	27 and 7	27 and 8	5 and 8	8.5999	8.6789	8.6838	0.0558	0.0566	0.0526
6	9, 2, and 33	2,10, and 32	3, 31, and 12	26 and 4	20 and 7	24 and 11	9.1600	9.1945	9.2833	0.0185	0.0547	0.0139

From the Fig. 9, case 6 provides nearly flat voltage profile with a minimum voltage of 0.9860 pu and a maximum voltage of 1.0148 pu compared to other cases.

C. COMPARISON WITH DEFAULT VOLT/VAr CONTROL SETTINGS OF SMART INVERTER

The proposed optimal oversize, dispatch, and control settings of the Volt/VAr functions of smart inverters for PVs and BESSs are compared with the default Volt/VAr control settings. Accordingly, the default Volt/VAr control points are set as v_1=0.92 pu, v_2=0.98 pu, v_3=1.02 pu, v_4=1.08 pu,and v_r=1 pu with an inverter oversize of 10 % [25]. Table 3 presents a comparison of the optimal Volt/VAr control settings with the default Volt/VAr control settings. Consequently, in case 6, the optimal Volt/VAr control setting maximizes the PVHC by 103.58 % and minimizes the voltage deviation by 72.26 % compared to the default Volt/VAr control settings.

D. COMPARISON WITH CONVENTIONAL METAHEURISTIC OPTIMIZATION METHODS

The performance of the proposed SMA optimization is compared with the existing conventional metaheuristic optimization methods (GA and PSO). For this comparison, GA with the population size and the maximum generations of 100, the crossover and mutation probability of 0.8 and 0.01, respectively were used [20]. Similarly, PSO with the population size and the maximum iteration of 100, acceleration factor (c_1 and c_2) of 2, and the inertia weight (ω_{max} and ω_{min}) of 0.4 and 0.9, respectively were used [19]. The results are summarized in Table 4 and from the comparison, it can be concluded that the SMA optimization methods can outperform GA and PSO in finding the globally optimal values in each cases.

V. CONCLUSION

Based on the advent of smart inverters that provide grid support functions, this paper proposed an optimal reactive power (Volt/VAr) control of the smart inverters for PVs and BESSs to improve the PVHC in distribution networks. The proposed method optimally coordinate PVs and BESSs smart inverter oversize, dispatch, and control settings to improve the PVHC of the distribution network. In addition, the optimal locations, sizes, and power dispatches of the PVs and BESSs were determined. The problem was formulated as a multi-objective mixed-integer nonlinear optimization to simultaneously maximize the PVHC and minimize the VD. The recent bio-inspired metaheuristic optimization method called SMA was used to solve the optimal solutions. Moreover, six test cases were simulated on an IEEE 33-node test system using MATLAB software. The simulation results showed that the proposed optimal Volt/VAr control of the smart inverters for both PVs and BESSs case maximize the PVHC and minimize the VD compared to other cases. Furthermore, the proposed method has superior performance compared to the default control setting of the Volt/VAr functions of the smart inverters and conventional metaheuristic optimization methods. In future work, the effects of optimal smart inverter settings on distribution network faults and the coordination of smart inverter with legacy active network management to improve PVHC will be studied.

REFERENCES

[1] T. Adefarati and R. C. Bansal, "Integration of renewable distributed generators into the distribution system: A review," *IET Renew. Power Gener.*, vol. 10, no. 7, pp. 873–884, Aug. 2016.

[2] T. Gush, S. B. A. Bukhari, R. Haider, S. Admasie, Y.-S. Oh, G.-J. Cho, and C.-H. Kim, "Fault detection and location in a microgrid using mathematical morphology and recursive least square methods," *Int. J. Electr. Power Energy Syst.*, vol. 102, pp. 324–331, Nov. 2018.

[3] L. Wang *et al.*, "Research on large-scale photovoltaic planning based on risk assessment in distribution network," *J. Electr. Eng. Technol.*, vol. 15, pp. 1107–1114, 2020, doi: 10.1007/s42835-020-00412-x.
[4] T. Gush, S. B. A. Bukhari, K. K. Mehmood, S. Admasie, J.-S. Kim, and C.-H. Kim, "Intelligent fault classification and location identification method for microgrids using discrete orthonormal stockwell transform-based optimized multi-kernel extreme learning machine," *Energies*, vol. 12, no. 23, p. 4504, Nov. 2019.
[5] G.-J. Cho, C.-H. Kim, Y.-S. Oh, M.-S. Kim, and J.-S. Kim, "Planning for the future: Optimization-based distribution planning strategies for integrating distributed energy resources," *IEEE Power Energy Mag.*, vol. 16, no. 6, pp. 77–87, Nov. 2018.
[6] *IEEE Standard for Interconnection and Interoperability of Distributed Energy Resources With Associated Electric Power Systems Interfaces*, Standard 1547-2018 (Revision of IEEE Std 1547-2003), 2018, pp. 1–138.
[7] X. Su, M. A. S. Masoum, and P. J. Wolfs, "Optimal PV inverter reactive power control and real power curtailment to improve performance of unbalanced four-wire LV distribution networks," *IEEE Trans. Sustain. Energy*, vol. 5, no. 3, pp. 967–977, Jul. 2014.
[8] M. Mohammadjafari, R. Ebrahimi, and V. P. Darabad, "Optimal energy management of a microgrid incorporating a novel efficient demand response and battery storage system," *J. Electr. Eng. Technol.*, vol. 15, no. 2, pp. 571–590, Mar. 2020.
[9] K. K. Mehmood, S. U. Khan, S. Lee, Z. M. Haider, M. K. Rafique, and C. Kim, "Optimal sizing and allocation of battery energy storage systems with wind and solar power DGs in a distribution network for voltage regulation considering the lifespan of batteries," *IET Renew. Power Gener.*, vol. 11, no. 10, pp. 1305–1315, Aug. 2017.
[10] A. Kumar, N. K. Meena, A. R. Singh, Y. Deng, X. He, R. Bansal, and P. Kumar, "Strategic integration of battery energy storage systems with the provision of distributed ancillary services in active distribution systems," *Appl. Energy*, vol. 253, Nov. 2019, Art. no. 113503.
[11] J. Hashimoto, T. S. Ustun, and K. Otani, "Smart inverter functionality testing for battery energy storage systems," *Smart Grid Renew. Energy*, vol. 8, no. 11, pp. 337–350, 2017.
[12] S. M. Ismael, S. H. E. Abdel Aleem, A. Y. Abdelaziz, and A. F. Zobaa, "State-of-the-art of hosting capacity in modern power systems with distributed generation," *Renew. Energy*, vol. 130, pp. 1002–1020, Jan. 2019.
[13] F. Ding and B. Mather, "On distributed PV hosting capacity estimation, sensitivity study, and improvement," *IEEE Trans. Sustain. Energy*, vol. 8, no. 3, pp. 1010–1020, Jul. 2017.
[14] F. Capitanescu, L. F. Ochoa, H. Margossian, and N. D. Hatziargyriou, "Assessing the potential of network reconfiguration to improve distributed generation hosting capacity in active distribution systems," *IEEE Trans. Power Syst.*, vol. 30, no. 1, pp. 346–356, Jan. 2015.
[15] S. Wang, S. Chen, L. Ge, and L. Wu, "Distributed generation hosting capacity evaluation for distribution systems considering the robust optimal operation of OLTC and SVC," *IEEE Trans. Sustain. Energy*, vol. 7, no. 3, pp. 1111–1123, Jul. 2016.
[16] P. H. Divshali and L. Söder, "Improving hosting capacity of rooftop PVs by quadratic control of an LV-central BSS," *IEEE Trans. Smart Grid*, vol. 10, no. 1, pp. 919–927, Jan. 2019.
[17] A. Ali, K. Mahmoud, D. Raisz, and M. Lehtonen, "Probabilistic approach for hosting high PV penetration in distribution systems via optimal oversized inverter with watt-var functions," *IEEE Syst. J.*, vol. 15, no. 1, pp. 684–693, Mar. 2021.
[18] J. F. B. Sousa, C. L. T. Borges, and J. Mitra, "PV hosting capacity of LV distribution networks using smart inverters and storage systems: A practical margin," *IET Renew. Power Gener.*, vol. 14, no. 8, pp. 1332–1339, Jun. 2020.
[19] S. K. Sahu and D. Ghosh, "Hosting capacity enhancement in distribution system in highly trenchant photo-voltaic environment: A hardware in loop approach," *IEEE Access*, vol. 8, pp. 14440–14451, 2020.
[20] S. Sakar, M. E. Balci, S. H. E. Abdel Aleem, and A. F. Zobaa, "Increasing PV hosting capacity in distorted distribution systems using passive harmonic filtering," *Electr. Power Syst. Res.*, vol. 148, pp. 74–86, Jul. 2017.
[21] G. W. Chang and N. Cong Chinh, "Coyote optimization algorithm-based approach for strategic planning of photovoltaic distributed generation," *IEEE Access*, vol. 8, pp. 36180–36190, 2020.
[22] P. Singh, N. K. Meena, A. Slowik, and S. K. Bishnoi, "Modified african buffalo optimization for strategic integration of battery energy storage in distribution networks," *IEEE Access*, vol. 8, pp. 14289–14301, 2020.
[23] A. Ali, K. Mahmoud, and M. Lehtonen, "Maximizing hosting capacity of uncertain photovoltaics by coordinated management of OLTC, VAr sources and stochastic EVs," *Int. J. Electr. Power Energy Syst.*, vol. 127, May 2021, Art. no. 106627.
[24] Y. M. Atwa, E. F. El-Saadany, M. M. A. Salama, and R. Seethapathy, "Optimal renewable resources mix for distribution system energy loss minimization," *IEEE Trans. Power Syst.*, vol. 25, no. 1, pp. 360–370, Feb. 2010.
[25] M. Rylander, H. Li, J. Smith, and W. Sunderman, "Default volt-var inverter settings to improve distribution system performance," in *Proc. IEEE Power Energy Soc. Gen. Meeting (PESGM)*, Jul. 2016, pp. 1–5.
[26] S. Li, H. Chen, M. Wang, A. A. Heidari, and S. Mirjalili, "Slime mould algorithm: A new method for stochastic optimization," *Future Gener. Comput. Syst.*, vol. 111, pp. 300–323, Oct. 2020.
[27] M. Mostafa, H. Rezk, M. Aly, and E. M. Ahmed, "A new strategy based on slime mould algorithm to extract the optimal model parameters of solar PV panel," *Sustain. Energy Technol. Assessments*, vol. 42, Dec. 2020, Art. no. 100849.
[28] M. E. Baran and F. F. Wu, "Network reconfiguration in distribution systems for loss reduction and load balancing," *IEEE Power Eng. Rev.*, vol. 9, no. 4, pp. 101–102, Apr. 1989.
[29] *Static Load Profiles*. Accessed: Sep. 8, 2020. [Online]. Available: http://origin.sce.com/regulatory/load-profiles/2019-static-load-profile%s
[30] *NREL Measurement and Data Center (MIDC) Solar Radiation Research Laboratory (SRRL) Baseline Measurement System (BMS)*. Accessed: Sep. 8, 2020. [Online]. Available: http://www.nrel.gov/midc/
[31] R. S. Rao, K. Ravindra, K. Satish, and S. V. L. Narasimham, "Power loss minimization in distribution system using network reconfiguration in the presence of distributed generation," *IEEE Trans. Power Syst.*, vol. 28, no. 1, pp. 317–325, Feb. 2013.
[32] M. M. Aman, G. B. Jasmon, A. H. A. Bakar, and H. Mokhlis, "Optimum network reconfiguration based on maximization of system loadability using continuation power flow theorem," *Int. J. Electr. Power Energy Syst.*, vol. 54, pp. 123–133, Jan. 2014.

TEKE GUSH (Graduate Student Member, IEEE) was born in Addis Ababa, Ethiopia. He received the B.S. degree in electrical engineering from the Addis Ababa Institute of Technology, Addis Ababa, in 2015. He is currently pursuing the Ph.D. degree with Sungkyunkwan University, Suwon, South Korea. His research interests include renewable energy grid integration, hosting capacity maximization of distribution networks, smart inverter application, power system protection, and artificial intelligence applications for the protection of microgrid and islanding detection.

CHUL-HWAN KIM (Senior Member, IEEE) received the B.S., M.S., and Ph.D. degrees in electrical engineering from Sungkyunkwan University, South Korea, in 1982, 1984, and 1990, respectively.

In 1990, he joined Cheju National University, Cheju, South Korea, as a Full-Time Lecturer. He was a Visiting Academician with the University of Bath, Bath, U.K., in 1996, 1998, and 1999. He has been a Professor with the College of Information and Computer Engineering, Sungkyunkwan University, since 1992, where he is currently the Director of the Center for Power Information Technology. His current research interests include power system protection, artificial intelligence applications for protection and control, modeling and protection of microgrid, and DC systems.

SAMUEL ADMASIE (Graduate Student Member, IEEE) received the B.S. degree in electrical engineering from the Addis Ababa Institute of Technology, Addis Ababa, Ethiopia, in 2015. He is currently pursuing the Ph.D. degree with Sungkyunkwan University, Suwon, South Korea. His research interests include DER integration and distribution systems planning, artificial intelligence applications for power system protection and islanding detection, power system optimization related to integration of renewables, and storage devices in distribution networks.

JI-SOO KIM (Graduate Student Member, IEEE) was born in South Korea, in 1992. He received the B.S. degree from the College of Information and Communication Engineering, Sungkyunkwan University, Republic of Korea, in 2016. He is currently pursuing the master's/Ph.D. degree. His research interests include power system transients, wind power generation, and distributed energy resource.

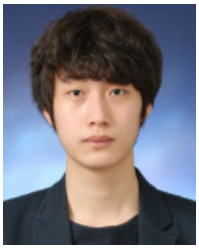

JIN-SOL SONG (Graduate Student Member, IEEE) received the B.S. degree from the College of Information and Communication Engineering, Sungkyunkwan University, Republic of Korea, in 2017. He is currently pursuing the master's/Ph.D. degree. His research interests include distributed generation and power system protection.